Room Temperature Operational Thermochromic Liquid Crystals

M. Seredyuk,[†] Ana B. Gaspar,*[,‡] V. Ksenofontov,[†] S. Reiman,[†] Y. Galyametdinov,[§] W. Haase,[||] E. Rentschler,[†] and P. Gütlich*[,†]

Institut für Anorganische und Analytische Chemie, Johannes-Gutenberg-Universität, Staudinger-Weg 9, D-55099 Mainz, Germany, Institut de Ciència Molecular/Departament de Química Inorgànica, Universitat de València, Doctor Moliner 50, 46100 Burjassot, València, Spain, Kazan Physical Technical Institute, Russian Academy of Science, Sibirsky Tract 10/7, 420029, Kazan, Russia, and Institute of Physical Chemistry, Darmstad University of Technology, Petersenstrasse 20, 64287, Darmstad, Germany

Received November 29, 2005. Revised Manuscript Received March 14, 2006

Thermochromic liquid crystals operating in the room temperature region have been successfully designed and synthesized. The reaction of 3,5-dialkoxy-*N*-4*H*-1,2,4-triazol-4-ylbenzamide ligands with $Fe(4\text{-}MeC_6H_4SO_3)_2$ salt have afforded a family of complexes with the general formula $[Fe(C_n\text{-trz})_3](4\text{-}MeC_6H_4SO_3)_2 \cdot H_2O$, *n* being the number of carbon atoms of the alkyl chain (8 (**1**), 10 (**2**), and 12 (**3**)). It appears that spin-crossover (SCO) behavior occurs in the temperature range at which the materials show a discotic columnar mesophase D_{hd}. As a result of the ability of liquid crystals to form thin layers, it is possible to obtain thermochromic SCO films. Understanding of possible interplay/synergy between the different phase transitions occurring in these materials is still a perspective study but certainly is exciting and attractive to chemists as well as physicists.

Introduction

Thermochromism is a well-know and useful property frequently observed in many different types of material.[1] The change of color with temperature is certainly a phenomenon which is of interest in the field of liquid crystals,[2] and many applications are based on this property: thermometers (fever indicators, gadgets, design applications, etc.) or warning signals (e.g., on heaters). While this type of color change has rarely been observed for nonchiral organic liquid crystals,[3] several papers have reported thermochromism in nonchiral metal-containing liquid crystals,[4] however, in many cases in a rather anecdotal fashion.[4] More successful has been the development of cholesteric liquid crystals[5] for the production of colored electrooptical films together with the liquid crystal organic light-emitting diodes.[6] Worth mentioning is also the achievement of photochromic liquid crystals.[7]

We have recently investigated the tailoring of multifunctional materials combining spin-crossover (SCO) and liquid crystalline (LC) behavior. SCO materials reversibly switch between a nearly diamagnetic low-spin (LS) state and a paramagnetic high-spin (HS) state under temperature variation, pressure, or light.[8] A sharp change of the structure, magnetism, color, and dielectric constant of the system in response to these stimuli may occur in the solid state. As a result of their switchable properties the SCO materials may potentially be useful for rewritable optical, thermal, or pressure memories at a nanometric scale.[8−11] The specific peculiarities of SCO and LC materials have stimulated the idea of combining both properties in a single material. Synergetic systems with two or more phase transitions of different physical nature may lead to a number of advantages in practical applications, for example, enhancement of spin transition signals, switching, and sensing in different temperature regimes.[2,12] A first step in this direction was done by Galyametdinov and co-workers, who reported an iron(III) complex combining both LC and SCO properties.[13] Both properties are not synchronous in that material and appear in different temperature regimes. Hayami and co-workers[14]

[†] Johannes-Gutenberg-Universität.
[‡] Universitat de València.
[§] Russian Academy of Science.
[||] Darmstad University of Technology.

(1) Granqvist, C. G. *Solid State Mater. Sci.* **1990**, *16*, 291 and references therein.
(2) (a) Serrano, J. L. *Metallomesogens*; VCH: New York, 1996 (and references therein). (b) Hudson, S. A.; Maitlis, P. M. *Chem. Rev.* **1993**, *93*, 861. (c) Donnio, B.; Bruce, D. W. *Struct. Bonding* **1999**, *95*, 193. (d) Lemieux, R. P. *Acc. Chem. Res.* **2001**, *34*, 845.
(3) Shvartsman, F. P.; Krongauz, V. A. *Nature (London)* **1984**, *309*, 608.
(4) (a) Bruce, D. W.; Dunmur, P. A.; Esteruelas, M. A.; Hunt, S. E.; Maitlis, P. M.; Marsden, J. R.; Sola, E.; Stacey, J. M. *J. Mater. Chem.* **1991**, *1*, 251. (b) Esteruelas, M. A.; Sola, E.; Oro, L. A.; Ros, M. B.; Serrano, J. L. *Chem. Commun.* **1986**, 55. (c) Ohta, K.; Hasabe, H.; Moriya, M.; Fujimoto, T.; Yamamoto, I. *J. Mater. Chem.* **1991**, *1*, 831. (d) Gregg, B. A.; Fox, M. A.; Bard, A. J. *J. Phys. Chem.* **1989**, *93*, 4227.
(5) De Filpo, G.; Nicoletta, F. P.; Chidichimo, G. *Adv. Mater.* **2005**, *17*, 1150.
(6) Aldred, M. P.; Contoret, A. E. A.; Farrar, S. R.; Stephen, M. K.; Mathieson, D.; O'Neill, M.; Tsoi, W. C.; Vlachos, P. *Adv. Mater.* **2005**, *17*, 1368.
(7) (a) Frogoli, M.; Mehl, G. H. *Chem. Phys. Chem.* **2003**, *1*, 101. (b) Irie, M. *Chem. Rev.* **2000**, *100*, 1685.
(8) Gütlich, P., Goodwin, H. A., Eds. Spin Crossover in Transition Metal Compounds. *Top. Curr. Chem.* **2004**, *233*−*235*.
(9) Real, J. A.; Gaspar, A. B.; Niel, V.; Muñoz, M. C. *Coord. Chem. Rev.* **2003**, *236*, 121.
(10) Real, J. A.; Gaspar, A. B.; Muñoz, M. C. *Dalton Trans.* **2005**, 2062−2079.
(11) Gütlich, P.; Hauser, A.; Spiering, H. *Angew. Chem., Int. Ed. Engl.* **1994**, *33*, 2024.
(12) Gaspar, A. B.; Ksenofontov, V.; Seredyuk, M.; Gütlich, P. *Coord. Chem. Rev.* **2005**, *249*, 2661.
(13) Galyametdinov, Y.; Ksenofontov, V.; Prosvirin, A.; Ovchinnikov, I.; Ivanova, G.; Gütlich, P.; Haase, W. *Angew. Chem., Int. Ed.* **2001**, *40*, 4269.

10.1021/cm052632w CCC: $33.50
Published on Web 04/18/2006

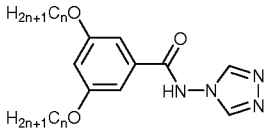

n = 8, 10, 12

(a)

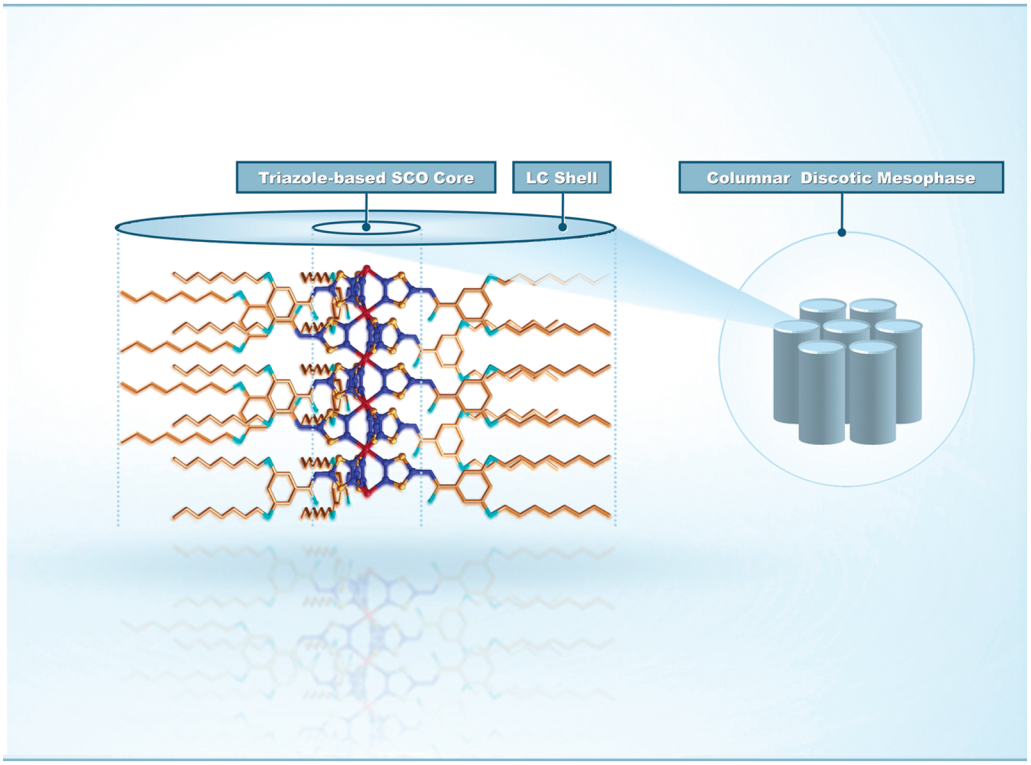

(b)

Figure 1. (a) Schematic drawings of the ligand 3,5-dialkoxy-*N*-4*H*-1,2,4-triazol-4-ylbenzamide and (b) of the structure of complexes $[Fe(C_n\text{-trz})_3](4\text{-}MeC_6H_4SO_3)_2{\cdot}H_2O$ (**1**−**3**), $[Zn(C_n\text{-trz})_3](4\text{-}MeC_6H_4SO_3)_2{\cdot}H_2O$ (**4**−**6**), and $[Fe(C_n\text{-trz})_3]$ $(4\text{-}MeC_6H_4SO_3)_2$ (**7**−**9**).

have recently observed a spin transition around 230 K in the mononuclear iron(II) complex $[Fe(3C16\text{-}L)_2(NCS)_2]$ (3C16-L: 3,4,5-tris(hexadecyloxy)-*N*-((pyridin-2-yl)methylene)benzenamine), which subsequently revealed the smetic phase above 350 K.

We have investigated the possibility to synchronize both transitions, the spin transition and crystal−liquid−crystal transition, in Fe(II) complexes, where SCO takes place between the $S = 0$ ($^1A_{1g}$) and the $S = 2$ ($^5T_{2g}$) states. The first step in the tailoring of these multifunctional materials has been the choice of SCO systems showing abrupt spin transition near or above room temperature. This is the range of temperatures at which usually the LC phase transition is observed. In this respect, the polymeric SCO compounds based on the triazole-based ligands are among the best candidates, showing abrupt spin transition above or near to room temperature accompanied by a pronounced change of color.[15,16] The second step in this approach concerns the incorporation of the LC moiety into the SCO system, which implies the attachment of the aromatic core with the alkyl chains to the triazole ligand (Figure 1). The mixture of 3,5-dialkoxy-*N*-4*H*-1,2,4-triazol-4-ylbenzamide ligands and $Fe(4\text{-}MeC_6H_4SO_3)$ salt have afforded a family of complexes with the general formula $[Fe(C_n\text{-trz})_3](4\text{-}MeC_6H_4SO_3)_2{\cdot}H_2O$, *n* being the number of carbon atoms of the alkyl chain (8 (**1**), 10 (**2**), and 12 (**3**); Figure 1). In a similar synthetic way the analogous systems with Zn(II), $[Zn(C_n\text{-trz})_3](4\text{-}MeC_6H_4SO_3)_2{\cdot}H_2O$ (**4**−**6**), have also been synthesized. These materials do not exhibit SCO properties and serve as reference systems in the study of SCO and LC properties in $[Fe(C_n\text{-trz})_3](4\text{-}MeC_6H_4SO_3)_2{\cdot}H_2O$ materials.

Experimental Section

Synthesis of Materials. Starting reagents and solvents were obtained commercially from Aldrich or Acros and used as received.

(14) Hayami, S.; Danjobara, K.; Inoue, K.; Ogawa, Y.; Matsumoto, N.; Maeda, Y. *Adv. Mater*. **2004**, *11*, 16.

(15) Kahn, O.; Kröber, J.; Jay, C. *Adv. Mater*. **1992**, *4*, 718.

(16) Kahn, O.; Martinez, C. J. *Science* **1998**, *279*, 44.

General Procedure for 3,5-Dialkoxybenzoic Acid. Potassium 3,5-dihydroxobenzoate (5.46 g, 28.4 mmol), 1-bromoalkane (85.2 mmol), anhydrous K_2CO_3 (7.88 g, 56.8 mmol), tetrabutylammonium bromide (0.3 g, 0.3 mmol), and a pinch of TiO_2 as a catalyst were mixed in a flask and heated for 2 h with stirring at 120 °C in solventless conditions. After cooling the product was extracted with $CHCl_3$ and filtered, and the solvent distilled off under reduced pressure. The resulting compound was suspended in a solution of KOH (4 g, 71.4 mmol) in an ethanol/water solution (19:1, 100 mL) and heated under reflux for 1 h. The reaction mixture was cooled to room temperature and brought to pH = 5 with 10% (v/v) formic acid. The 3,5-dialkoxybenzoic acid precipitated upon further cooling was filtered and then recrystallized from hot ethanol before being dried in vacuo to yield a white crystalline solid. Yield 50−60%.

3,5-Dioctyloxybenzoic Acid. ^{1}H NMR (400 MHz, $CDCl_3$): δ 7.25 (2H, d, J = 2.3 Hz, Ar*H*), 6.71 (1H, d, J = 2.3 Hz, Ar*H*), 4.00 (4H, t, J = 7.0 Hz, O−CH_2), 1.81 (4H, quint, J = 7.0 Hz, O−CH$_2$−CH_2), 1.48−1.35 (20H, m, $(CH_2)_5$), 0.92 (6H, t, J = 7.0 Hz, CH_3).

3,5-Didecyloxybenzoic Acid. ^{1}H NMR (400 MHz, $CDCl_3$): δ 7.24 (2H, d, J = 2.3 Hz, Ar*H*), 6.70 (1H, d, J = 2.3 Hz, Ar*H*), 4.00 (4H, t, J = 7.0 Hz, O−CH_2), 1.82 (4H, quint, J = 7.0 Hz, O−CH$_2$−CH_2), 1.49−1.35 (28H, m, $(CH_2)_7$), 0.90 (6H, t, J = 7.0 Hz, CH_3).

3,5-Didodecyloxybenzoic Acid. ^{1}H NMR (400 MHz, $CDCl_3$): δ 7.23 (2H, d, J = 2.3 Hz, Ar*H*), 6.71 (1H, d, J = 2.3 Hz, Ar*H*), 3.98 (4H, t, J = 7.0 Hz, O−CH_2), 1.81 (4H, quint, J = 7.0 Hz, O−CH$_2$−CH_2), 1.49−1.35 (36H, m, $(CH_2)_9$), 0.90 (6H, t, J = 7.0 Hz, CH_3).

Diphenyl(2,3-dihydro-2-thioxo-3-benzoxazoleyl)phosphate. To a solution of 2-benzoxazolethiol (4.53 g, 30 mmol) and triethylamine (4.2 mL, 30 mmol) in benzene (35 mL) was added dropwise at room temperature with stirring a solution of diphenyl phosphochloridate (6.2 mL, 30 mmol) in benzene (10 mL). The addition was completed in 30 min, and stirring was continued at room temperature for an additional 1.5 h. Triethylamine hydrochloride was removed by filtration, and the solvent was distilled off in vacuo. The syrup-like residue was dissolved with stirring in boiling *n*-hexane, and the turbid solution was decanted and placed in a refridgerator overnight. The procedure was repeated several times to provide colorless or slightly violet block crystals. Yield 5.9 g (52%).

MS-EI (relative intensity): 383.0 $[M]^+$ (100%). ^{1}H NMR (400 MHz, $CDCl_3$): δ 7.41−7.23 (14H, m). ^{13}C ($CDCl_3$, 100 MHz): δ 180.11 (C═S), 148.29, 147.40, 131.78, 131.71, 125.90, 125.30, 123.89, 114.64, 109.97. FT-IR (KBr; cm^{-1}): υ (P═O) 1284, υ (C−O−P) 1178, 979. Anal. Calcd for $C_{19}H_{14}NO_4PS$: C, 59.53; H, 3.68; N, 3.65; S, 8.36. Found: C, 59.40; H, 3.16; N, 3.74; S, 8.39.

3,5-Dialkoxy-*N*-4*H*-1,2,4-triazol-4-ylbenzamide. To a batch of 4-amino-1,2,4-triazole (1 g, 11.89 mmol) was added at room temperature a tetrahydrofuran solution of a mixture of the corresponding dialkobenzoic acids (15.47 mmol), triethylamine (1.56 g, 15.47 mmol), and diphenyl(2,3-dihydro-2-thioxo-3-benzoxazoleyl)phosphate (5.9 g, 15.47 mmol). The mixture was refluxed for 2 h and allowed to cool at room temperature. The resulting solution was evaporated to dryness to provide a viscous oil, which was dissolved in chloroform (10 mL) and placed in a refridgerator overnight resulting in precipitation of unutilized 4-amino-1,2,4-triazole. The mixture was filtered, and the filtrate was subjected to column chromatography using $CHCl_3$/MeOH (gradient from 100/0 to 97/3) as the eluent. The second fraction was collected and evaporated to dryness to provide 3,5-dialkoxy-*N*-4*H*-1,2,4-triazol-4-ylbenzamide as a white waxy solid that was then recrystallized from methanol. Yield 70−80%.

3,5-Dioctyloxy-*N*-4*H*-1,2,4-triazol-4-ylbenzamide. ^{1}H NMR (400 MHz, $CDCl_3$): δ 8.20 (2H, s, Trz*H*), 7.17 (2H, d, J = 2.0 Hz, Ar*H*), 6.63 (1H, t, J = 2.0 Hz, Ar*H*), 3.98 (4H, t, J = 7.0 Hz, OCH_2), 1.77 (4H, m, J = 7.0 Hz, OCH$_2$CH_2), 1.48−1.36 (20H, m, $(CH_2)_5$), 0.88 (6H, t, J = 7.0 Hz, CH_3). FT-IR (KBr; cm^{-1}): 3116, 2923, 2853, 1671, 1605, 1329, 1169, 1072, 856, 714, 626. Anal. Calcd for $C_{25}H_{40}N_4O_3$: C, 67.53; H, 9.07; N, 12.60. Found: C, 67.51; H, 9.16; N, 12.55.

3,5-Didecyloxy-*N*-4*H*-1,2,4-triazol-4-ylbenzamide. ^{1}H NMR (400 MHz, $CDCl_3$): δ 8.20 (2H, s, Trz*H*), 7.11 (2H, d, J = 2.0 Hz, Ar*H*), 6.69 (1H, t, J = 2.0 Hz, Ar*H*), 3.98 (4H, t, J = 7.0 Hz, OCH_2), 1.77 (4H, m, J = 7.0 Hz, OCH$_2$CH_2), 1.48−1.32 (28H, m, $(CH_2)_7$), 0.89 (6H, t, J = 7.0 Hz, CH_3). FT-IR (KBr; cm^{-1}): 3116, 2921, 2851, 1671, 1605, 1329, 1169, 1073, 856, 714, 628. Anal. Calcd for $C_{29}H_{48}N_4O_3$: C, 69.56; H, 9.66; N, 11.19. Found: C, 68.85; H, 9.31; N, 12.24.

3,5-Didodecyloxy-*N*-4*H*-1,2,4-triazol-4-ylbenzamide. ^{1}H NMR (400 MHz, $CDCl_3$): δ 8.23 (2H, s, Trz*H*), 7.17 (2H, d, J = 2.0 Hz, Ar*H*), 6.69 (1H, t, J = 2.0 Hz, Ar*H*), 3.98 (4H, t, J = 7.0 Hz, OCH_2), 1.77 (4H, m, J = 7.0 Hz, OCH$_2$CH_2), 1.48−1.35 (36H, m, $(CH_2)_9$), 0.88 (6H, t, J = 7.0 Hz, CH_3). FT-IR (KBr; cm^{-1}): 3115, 2921, 1851, 1729, 1670, 1604, 1329, 1169, 1074, 856, 714, 628. Anal. Calcd for $C_{33}H_{56}N_4O_3$: C, 71.18; H, 10.14; N, 10.06. Found: C, 71.19; H, 10.02; N, 10.05.

Synthesis of 1−6. To a hot methanolic solution of 3,5-dialkoxy-*N*-4*H*-1,2,4-triazol-4-ylbenzamide was added a methanolic solution of the M(4-Me$C_6H_4SO_3)_2$ ($^1/_3$ equiv, M = Zn or Fe). The mixture was refluxed for 5 min, then concentrated by evaporating, and allowed to cool to room temperature. The precipitate of a complex was filtered off and dried in air. Yield 60−80%.

1. FT-IR (KBr; cm^{-1}): 3094, 2926, 2855, 1697, 1605, 1216, 1164, 1124, 1033, 1009, 854, 813, 684, 628, 567. Anal. Calcd for $C_{89}H_{136}FeN_{12}O_{16}S_2$: C, 61.08; H, 7.83; N, 9.60; S, 3.66. Found: C, 61.43; H, 7.98; N, 9.60; S, 3.78.

2. FT-IR (KBr; cm^{-1}): 3095, 2924, 2854, 1696, 1606, 1215, 1164, 1125, 1034, 1010, 854, 812, 685, 629, 569. Anal. Calcd for $C_{101}H_{160}FeN_{12}O_{16}S_2$: C, 63.23; H, 8.41; N, 8.76; S, 3.34. Found: C, 63.93; H, 8.81; N, 8.51; S, 3.48.

3. FT-IR (KBr; cm^{-1}): 3096, 2923, 2853, 1696, 1605, 1217, 1164, 1125, 1034, 1009, 857, 812, 684, 628, 568. Anal. Calcd for $C_{113}H_{184}FeN_{12}O_{16}S_2$: C, 65.04; H, 8.89; N, 8.05; S, 3.07. Found: C, 65.44; H, 8.71; N, 7.69; S, 3.29.

4. FT-IR (KBr; cm^{-1}): 3114, 2925, 2854, 1697, 1605, 1210, 1168, 1124, 1034, 1010, 856, 812, 684, 628, 570. Anal. Calcd for $C_{89}H_{136}N_{12}O_{16}S_2Zn$: C, 60.75; H, 7.79; N, 9.55; S, 3.64. Found: C, 60.93; H, 8.02, 9.92; S, 3.68.

5. FT-IR (KBr; cm^{-1}): 3100, 2923, 2853, 1698, 1604, 1210 (as h), 1165, 1124, 1034, 1009, 858, 814, 683, 626, 568. Anal. Calcd for $C_{101}H_{160}N_{12}O_{16}S_2Zn$: C, 62.92; H, 8.36; N, 8.72; S, 3.39. Found: C, 63.21; H, 8.87; N, 8.53; S, 3.32.

6. FT-IR (KBr; cm^{-1}): 3100, 2923, 2853, 1699, 1605, 1210, 1167, 1124, 1033, 1009, 857, 817, 683, 627, 567. Anal. Calcd for $C_{113}H_{184}N_{12}O_{16}S_2Zn$: C, 64.74; H, 8.85; N, 8.02; S, 3.06. Found: C, 65.21; H, 9.31, N, 7.87; S, 2.88.

Magnetic Susceptibility Measurements. The variable-temperature magnetic susceptibility measurements were performed by using a Quantum Design MPMS2 SQUID susceptometer equipped with a 5.5 T magnet and operating at 1 T and 1.8−400 K. Experimental data were corrected for diamagnetism using Pascal's constants.

Mössbauer Spectroscopy. ^{57}Fe Mössbauer spectra were recorded using a constant-acceleration conventional spectrometer and helium bath cryostat or nitrogen cryostat. The sample and the Mössbauer source ^{57}Co/Rh were immersed in liquid helium to record the spectra

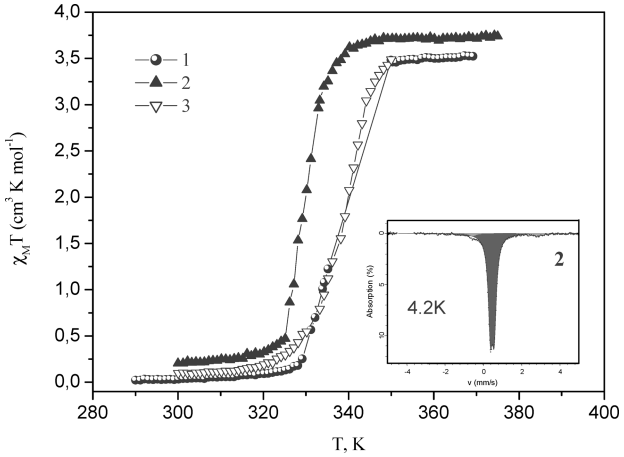

Figure 2. Magnetic properties of the complexes **1**−**3** in the form of $\chi_M T$ vs T recorded at a rate of 1 K/min. Inset: Mössbauer spectra of complex **2** acquired at 4.2 K, dark gray doublet (LS), and light gray doublet (HS). HS population (%), 4.76; IS_{HS}, 1.15(3) mm/s; ΔE_{QHS}, 3.38(6) mm/s; LS population (%), 95.24; IS_{LS}, 0.48(1) mm/s; ΔE_{QLS}, 0.20(1) mm/s. For complexes **1** and **3** the Mössbauer parameters at 4.2 K are as follows: HS population (%), 9.29 (**1**) and 0 (**3**); IS_{HS}, 1.18(1) mm/s (**1**); ΔE_{QHS}, 3.262-(2) mm/s (**1**); LS population (%), 90.71 (**1**) and 100 (**3**); IS_{LS}, 0.47(1) mm/s (**1**) and 0.47(3) mm/s (**3**); ΔE_{QLS}, 0.20(1) mm/s (**1**) and 0.20(2) mm/s (**3**).

at 4.2 K. The Recoil 1.03a Mössbauer Analysis Software was used to fit the experimental spectra.

Polarizing Optical Microscopy. The temperatures and textures of phase transitions were determined with a polarization microscope, equipped with a hot stage and with a temperature control of better than ±0.5 K.[13]

X-ray Powder Diffraction (XRD). X-ray measurements where obtained with a STOE STADI 2 diffractometer, equipped with a linear position-sensitive detector (STOE mini PSD). Monochromatic Cu Kα radiation was obtained by using a curved germanium detector (111 plane).

Differential Scanning Calorimetry (DSC) Measurements. DSC measuremnts were performed on a Mettler model DSC 822e. DSC profiles were recorded at the rate of 7 or 5 K/min and analyzed with a Mettler model STARe system. The samples were located in sealed sample pans.

Results and Discussion

Magnetic Properties of 1−3. The magnetic properties of **1-3** in the form of $\chi_M T$ versus T, χ_M being the molar susceptibility and T being the temperature, are depicted in Figure 2. At 300 K the values of 0.03 (**1**) cm^3 K mol^{-1}, 0.20 (**2**) cm^3 K mol^{-1}, and 0.10 (**3**) cm^3 K mol^{-1} indicate that these complexes are in the LS state. Mössbauer spectra recorded at 4.2 K confirm that the residual HS fraction does not exceed more than 10% of iron(II) ions in all materials (inset, Figure 2). Upon heating $\chi_M T$ increases abruptly within a few kelvin, attaining the values of 3.53 (**1**) cm^3 K mol^{-1}, 3.74 (**2**) cm^3 K mol^{-1}, and 3.47 (**3**) cm^3 K mol^{-1} at 346, 342, and 359 K, respectively. This clearly indicates the occurrence of SCO behavior, which additionally is accompanied by a pronounced change of color [from purple (LS state) to white (HS state); Figure 3]. The characteristic temperatures $T_{1/2}$ at which 50% of the molecules are in the LS and HS states, respectively, are 330 K (**2**) and 340 K for **1** and **3**. Thermogravimetric analysis (TGA) experiments have shown that dehydration takes place in the same temperature region where SCO occurs (Supporting Information). Dehydration of the materials is accomplished at around 360 K for **1,** 350 K for **2**, and 370 K in the case of **3**. Synergy between dehydration and SCO as observed in these materials has been reported in several cases.[8,15] It should be noted here that the magnetic properties of dehydrated materials have been also investigated and are reported below (Figure 6).

Temperature-Dependent XRD for 1−6. XRD spectra of the complexes **1**−**6** have been measured in the 300−375 K temperature region and at 230 K (Figure 4). The XRD patterns of the mesophase in most of the complexes gave a series of reflections with d spacing which could be indexed as belonging to a two-dimensional hexagonal lattice. Only in the pattern of **4** are some additional narrow reflexes in the region of $1/d = 0.17-0.25$ observed. All patterns also gave a halo at $d \sim 4.4$ Å ($1/d \sim 0.23$ Å^{-1}) which corresponds to the melt of the alkyl chains. On the basis of these findings a disordered discotic columnar mesophase D_{hd} has been identified in all the cases with the lattice constants a (298 K) shown in Table 1.

DSC and Optical Polarizing Microscopy Experiments for 1−6. To identify the thermotropic LC mesomophism of **1**−**6**, a polarizing optical microscopy apparatus was used. For all complexes, a discotic columnar mesophase at 230 K has been identified. On warming, isotropization occurs near 500 K, where the clearing points are $T_c = 490$ K (**1**), 488 K (**2**), 480 K (**3**), 497 K (**4**), 491 K (**5**), and 485 K (**6**). Realization of the crystalline state on these materials is difficult; in fact, no melting point has been observed.

DSC experiments performed at a rate of 7 K/min, in the warming mode, are shown in Figure 5. For compound **1**, broad peaks are observed at temperatures of $T_1 = 329$ K, $T_2 = 353$ K, $T_3 = 381$ K, $T_4 = 489$ K, and $T_5 = 589$ K. The thermal dependence of the heat flow for **2** and **3** is similar

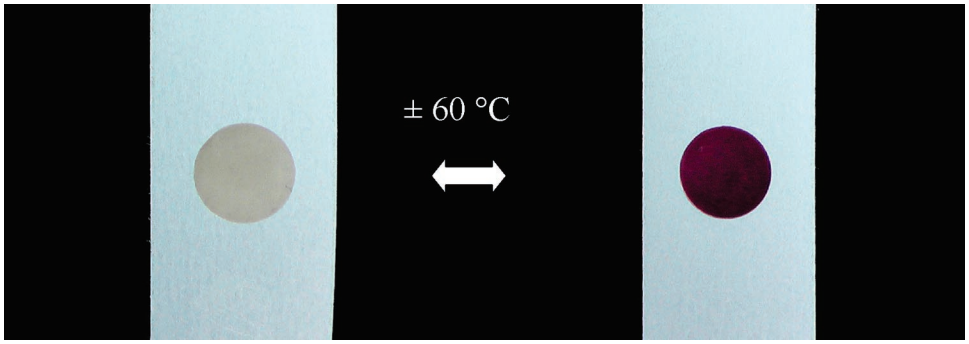

Figure 3. Change of color in the SCO LC films around 60 °C.

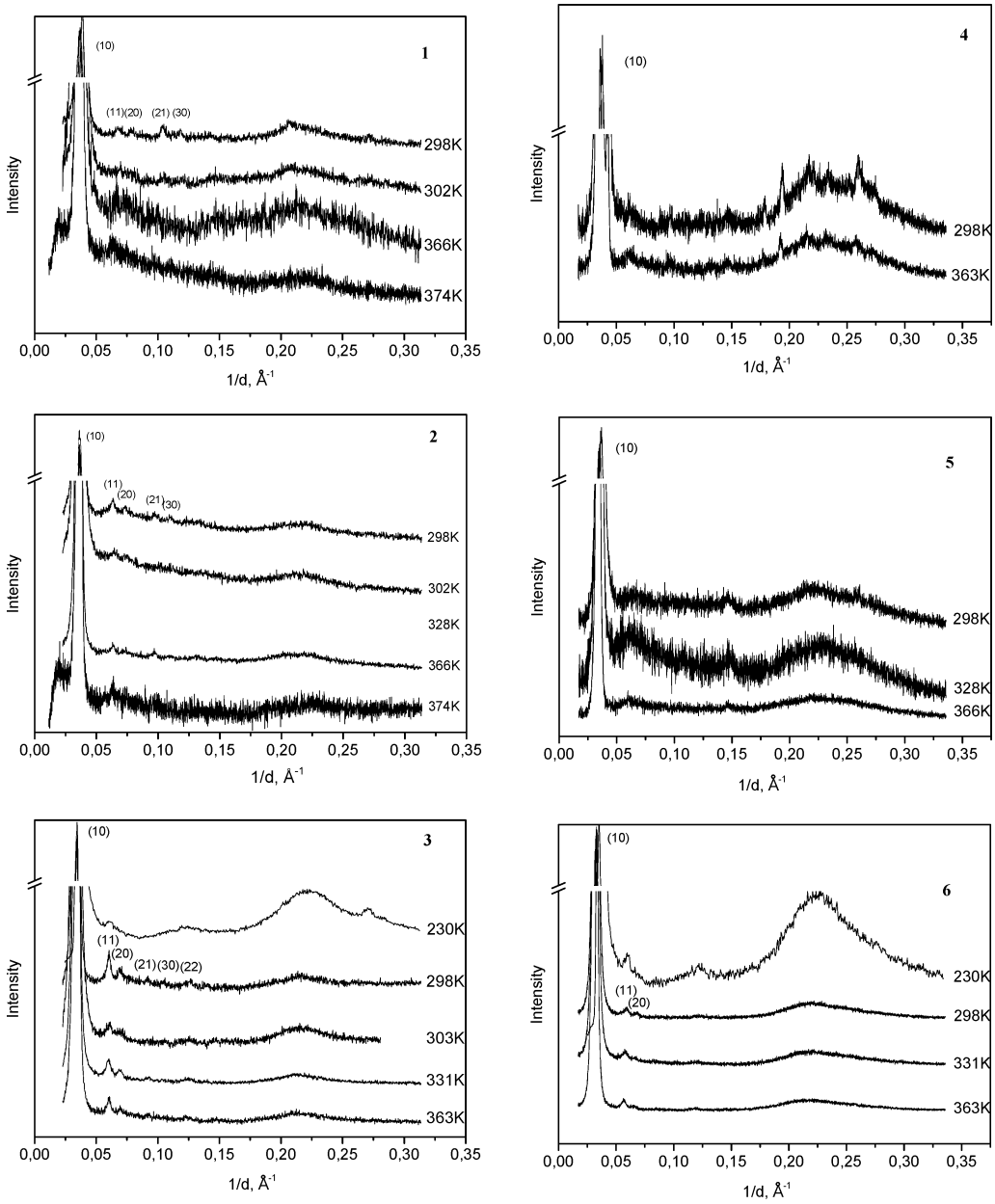

Figure 4. XRD patterns of complexes **1**−**3** (right) and **4**−**6** (left) at different temperatures (K).

Table 1. Thermal Dependence of the Interlayer Distances and Lattice Constant *a* in Å for 1−6

	T, K	$d_{interlayer}$, Å	*a*, Å		*T*, K	$d_{interlayer}$, Å	*a*, Å
1	298	25.9	29.9	**4**	298	26.4	30.5
	302	25.7	29.6		363	27.7	32.0
	366	27.1	31.2				
	374	27.7	32.0				
2	298	27.1	31.3	**5**	298	27.4	31.7
	302	27.6	31.8		328	28.4	32.8
	328	28.0	32.3		366	29.2	33.7
	366	28.6	33.0				
	374	29.2	33.7				
3	230	28.2	32.6	**6**	230	28.2	32.6
	298	29.0	33.5		298	28.6	33.0
	303	29.2	33.7		331	30.5	35.2
	331	29.4	33.9		363	31.0	35.8
	374	31.2	36.0				

to that of **1** despite the fact that in these compounds two peaks are observed in the 300−385 K temperature interval. Anomalies are observed at $T_1 = 327$ K, $T_2 = 351$ K, $T_4 = 486$ K, and $T_5 = 583$ K in **2** and at $T_1 = 349$ K, $T_2 = 377$ K, $T_4 = 489$ K, and $T_5 = 589$ K in the case of **3**. The peaks located at temperatures T_1, T_2, and T_3 correspond to the SCO and dehydration processes, which match exactly with the reported magnetic and TGA data. T_4 and T_5 are assigned to the isotropization and decomposition temperatures, respectively, as has been well-confirmed by optical polarizing microscopy and TGA analysis. For the complexes **4**−**6**, the peaks observed at $T_1 = 333$ K (**4**), 343 K (**5**), and 328 K (**6**) correspond to the dehydration processes. The anomalies in the heat flow observed at $T_4 = 479$ K (**4**), 479 K (**5**), and 476 K (**6**) and at $T_5 = 581$ K (**4**−**6**) are assigned to the isotropization and decomposition temperatures, respectively. Table 2 summarizes the derived thermodynamic parameters ΔH_{SCO} and ΔS_{SCO} together with ΔH_{DH} for the compounds **1**−**3**; the values are in the range of the values expected for Fe(II) compounds.[8,17] DSC measurements performed at a rate of 5 K/min between 175 and 400 K, in the cooling and

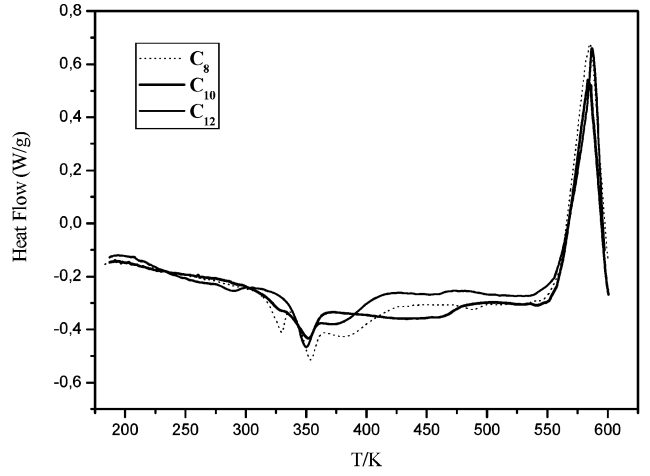

(a)

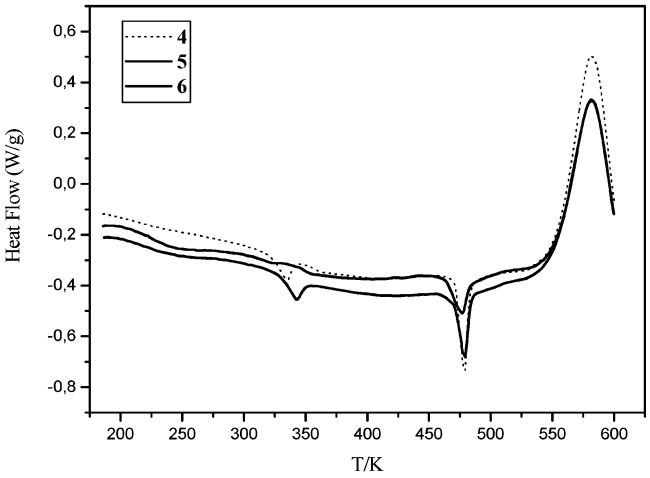

(b)

Figure 5. DSC data of complexes **1**−**3** (a) and **4**−**6** (b) in the warming mode recorded at the rate of 7 K/min.

Table 2. Thermodynamic Parameters of the SCO and Dehydration Processes

	ΔH_{DH}, kJ mol^{-1}	ΔH_{SCO}, kJ mol^{-1}	ΔS_{SCO}, J mol^{-1} K^{-1}
1	4.5	14.5	42.7
2	5.0	15.0	45.5
3	4.0	16.6	48.8

warming modes, have proved the reversibility of the processes (Supporting Information).

An interesting and important feature is the possibility to obtain these materials in the form of thin films. Approximately 10 mg of a complex were dissolved in $CHCl_3$ (1 mL), and subsequently the solution was layered onto a glass plate and the solvent was allowed to evaporate (Figure 3). A reversible change between purple (LS state) and white (HS state) coloration of the films by heating or cooling around 60 °C was observed without fatigue under sealed conditions.

(17) (a) Ksenofontov, V.; Gaspar, A. B.; Levchenko, G.; Fitzsimmons, B.; Gütlich, P. *J. Phys. Chem. B.* **2004**, *108*, 7723. (b) Niel, V.; Martinez-Agudo, J. M.; Muñoz, M. C.; Gaspar, A. B.; Real, J. A. *Inorg. Chem.* **2001**, *40*, 3838. (c) Moliner, N.; Gaspar, A. B.; Muñoz, M. C.; Niel, V.; Cano, J.; Real, J. A. *Inorg. Chem.* **2001**, *40*, 3986.

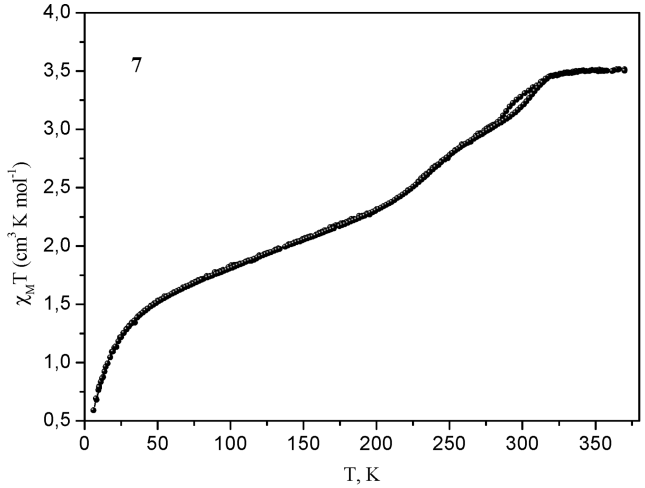

(a)

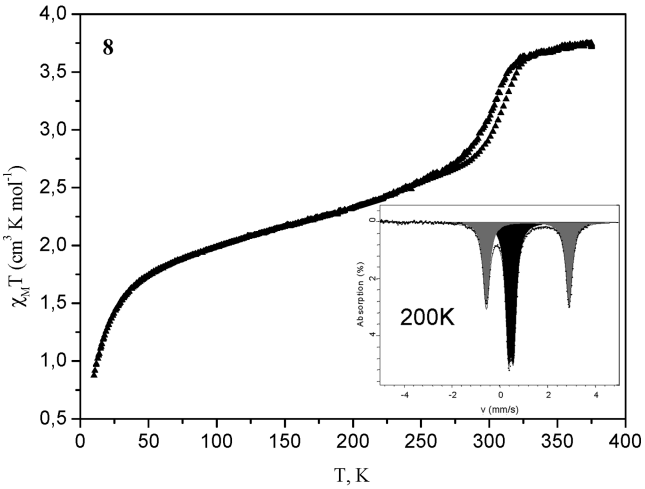

(b)

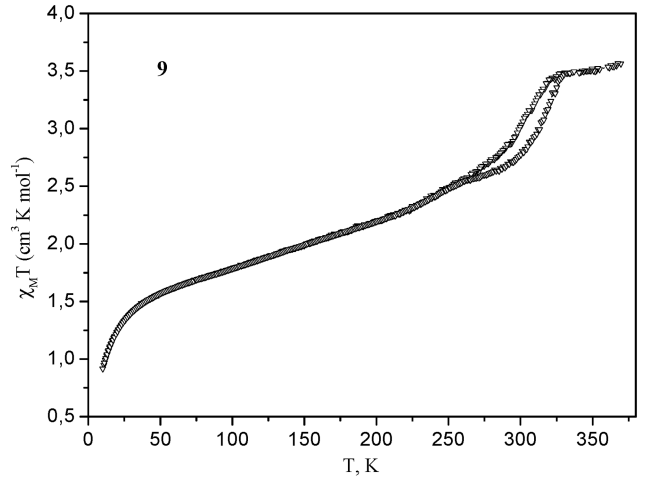

(c)

Figure 6. Magnetic properties of complexes **7**−**9** in the form of $\chi_M T$ vs T recorded at the rate of 1 K/min. Inset: Mössbauer spectra of complex **8** recorded at 200 K, dark gray doublet (LS), and light gray doublet (HS). HS population (%), 48.1; IS_{HS}, 1.14(1) mm/s; ΔE_{QHS}, 3.38(2) mm/s; LS population (%), 51.9; IS_{LS}, 0.44(1) mm/s; ΔE_{QLS}, 0.22(1) mm/s.

Magnetic Properties for 7−9. The magnetic properties of the dehydrated complexes $[Fe(C_n\text{-trz})_3](4\text{-}MeC_6H_4SO_3)_2$ (n = 8 (**7**), 10 (**8**), and 12 (**9**)) have been investigated (Figure 6). Dehydration of the complexes occurs upon heating the

samples from 300 K up to 400 K. Subsequently, the magnetic susceptibility of the dehydrated samples was recorded from 375 K down to 10 K and up to 375 K. The complexes reveal an incomplete and abrupt SCO behavior accompanied by hysteresis and color change [from purple (LS state) to white (HS state)] in the temperature region of 250−300 K. Around 50% of the Fe(II) ions have changed the electronic configuration as can be inferred from the value of $\chi_M T$ at 200 K. In fact, Mössbauer spectra recorded for compound **8** at 200 K have demonstrated that 50% of the iron(II) ions are in the LS state (Figure 6). Further decrease of the $\chi_M T$ value below 100 K, particularly below 50 K, is due to the zero field splitting (ZFS) of the iron atoms remaining in the HS state. Several measurements of the hysteresis cycles in **7**−**9** have confirmed their stability. It is worth noting that the abruptness of the spin transition and the hysteresis width increase upon increasing the length of the alkyl chain. Another remarkable fact is the incompleteness of the spin transition which became frozen below 200 K. A residual HS fraction of approximately 50% is unusual.[8]

Discussion. XRD on the complexes $[Fe(C_n\text{-trz})_3](4\text{-}MeC_6H_4\text{-}SO_3)_2 \cdot H_2O$ (**1**−**3**) in the temperature range of 370−230 K points out a decrease of interlayer distances of approximately 2 Å (Table 1), which could favor the LS configuration of the Fe(II) centers and could be connected to the structural variations occurring inside the mesophase, which have also been observed for the compounds $[Zn(C_n\text{-trz})_3](4\text{-}MeC_6H_4\text{-}SO_3)_2 \cdot H_2O$ (**4**−**6**; Table 1). Probably, such structural variations occurring in the discotic columnar mesophase are driving the SCO process in the compounds **1**−**3** and **7**−**9**, or it is just a coincidence that thermal SCO occurs in the same temperature range. An extensive XRD analysis between 200 and 375 K, in the warming and cooling modes, would be helpful to clarify this interesting question. Several authors[18,19] have concluded that the phase transition from the crystalline state to liquid crystal drives the SCO process in Fe(II) complexes. This, however, still remains as an open question, because it has not yet been confirmed experimentally.

(18) Fujigaya, T.; Jiang, D. L.; Aida, T. *J. Am. Chem. Soc.* **2003**, *125*, 14690.
(19) Bodenthin, Y.; Pietsch, U.; Möhwald, H.; Kurth, D. G. *J. Am. Chem. Soc.* **2005**, *127*, 3110.

Materials **7**−**9** can be prepared as thin films by heating films **1**−**3** up to 330 K under ambient conditions. Despite the fact that only 50% of the iron(II) atoms show SCO behavior, the color change is perfectly detectable and reversible after many cycles. The water reabsorption process has been investigated and shows that the materials recover the water molecules in an open atmosphere within 10 days (Supporting Information).

Conclusion. In summary, thermochromic liquid crystals operating in the room-temperature region have been synthesized. It appears that SCO behavior occurs in the temperature range at which the materials show a discotic columnar mesophase. As a result of the ability of liquid crystals to form thin layers it is possible to obtain SCO films. Understanding of possible interplay/synergy between the different phase transitions occurring in these materials is still a perspective study by chemists and physicists. We expect that the electrical field should be a suitable physical variable influencing the spin state in these multifunctional materials. The influence of an electrical field on the SCO process is currently being pursued in our group.

Acknowledgment. The authors wish to express their gratitude to Dr. H. Ehrenberg of the Darmstadt University of Technology, Darmstadt, for his help in carrying out XRD measurements. Ms. E. Muth and Ms. P. Räder of the Max-Planck-Institute for Polymer Research, Mainz, are also thanked for their help in performing TGA and DSC measurements. A.B.G. thanks the financial assistance from Alexander von Humboldt Foundation and the Spanish MEC for a Ramon y Cajal research contract and Project No. CTQ2004-03456-BQU. Y.G. acknowledges the financial support from the DLR/BMBF Project No. RUS 05/003 and RFBR Grant 03-03-32571. We also acknowledge the financial help from the Deutsche Forschungsgemeinschaft (Priority Program 1137 "Molecular Magnetism"), the Fonds der Chemischen Industrie, and the Materialwissenschaftliches Forschungszentrum der Universität Mainz.

Supporting Information Available: TGA analysis and DSC data of complexes **1**−**6** and magnetic susceptibility measured as a function of time for materials **7**−**9** (PDF). This material is available free of charge via the Internet at http://pubs.acs.org.

CM052632W